Available online at www.sciencedirect.com
SCIENCE DIRECT®
PERGAMON
Chaos, Solitons and Fractals 18 (2003) 829–841
CHAOS SOLITONS & FRACTALS
www.elsevier.com/locate/chaos

# Erosion of the safe basin for the transversal oscillations of a suspension bridge

Mário S.T. de Freitas [a,*,1], Ricardo L. Viana [a], Celso Grebogi [b]

[a] *Departamento de Física, Universidade Federal do Paraná, C.P. 19081, 81531-990, Curitiba, Paraná, Brazil*
[b] *Instituto de Física, Universidade de São Paulo, C.P. 66318, 05315-970, São Paulo, Brazil*

Accepted 20 February 2003

**Abstract**

The time evolution of the lowest order transversal oscillation mode of a suspension bridge is studied by means of a piecewise-linear forced and damped one-dimensional oscillator, in which the loss of smoothness is due to the asymmetric response of the bridge hangers with respect to stretching and compression. If the midpoint roadbed deflection is outside a specified safe region, the bridge is supposed to collapse. We analyze the relative area of the safe basin, or the fraction of initial conditions in the phase space for which the bridge does not collapse with respect to the damping and forcing parameters. The safe basin erosion is enhanced by the appearance of incursive fingers caused by the exponential accumulation of safe basin lobes towards an invariant manifold of a periodic orbit which undergoes a homoclinic bifurcation.


## 1. Introduction

The effects of wind-induced periodic forcing on structures were dramatically illustrated by the collapse of the Tacoma Narrows bridge in November 7, 1940. The elementary textbook explanation for this phenomenon addresses the linear resonance between the frequency of the staggered wind-induced Von Kármán vortices and the bridge natural frequency [1]. However, since linear resonance turns out to be a rather narrow phenomenon, it is unlikely to occur in an irregularly changing environment, hence the ultimate cause for the suspension bridge collapse should be investigated in the realm of non-linear phenomena [2].

The Tacoma Narrows bridge, prior to its collapse, was designed to have a slender, light and flexible roadbed, what allowed large-amplitude transversal vibrations. Generally, in a suspension bridge, the hangers which connect the roadbed to the main suspension cable, respond in an asymmetric way to transversal oscillations of the roadbed: they strongly resist to stretching but do not to compression (one-sided springs). This leads to a piecewise linear stiffness for the hangers, and the roadbed dynamics has features similar to periodically forced non-linear oscillators, including harmonic, quasiperiodic, and even chaotic motion.

Another point, where non-linear phenomena are relevant in the analysis of this problem, is that torsional oscillations were also observed just before the bridge collapse, as shown by the famous movie shot in the moment of the disaster [3]. Coupling between different vibration modes is a typical non-linear feature [4]. For those reasons, the oscillations of a suspension bridge represent a mechanical system with discontinuities, for which there is a reasonable amount of literature [5–10].

* Corresponding author.
[1] Permanent address: Departamento de Física, Centro Federal de Educação Tecnológica do Paraná, Curitiba, PR, Brazil.

0960-0779/03/$ - see front matter © 2003 Published by Elsevier Science Ltd.
doi:10.1016/S0960-0779(03)00035-3

In the Tacoma Narrows bridge disaster, the failure was ultimately caused by torsional oscillations, being triggered by the escape of a hanger out of its roadbed connection due to the large-amplitude transversal vibrations. Hence, we can reasonably assume the bridge to collapse if the transversal deflection exceeds some prespecified threshold. Moreover, we will consider the first transversal vibration mode for the bridge roadbed, in order to take the roadbed deflection at its midpoint as the maximum deformation for safety reasons. According to Refs. [2] and [11], we isolate and analyze the time evolution of the lowest vibrational mode by means of an initial value problem for a system of ordinary differential equations. Due to the piecewise-linear stiffness of the combined roadbed-hanger system, it boils down to a non-smooth forced and damped one-dimensional oscillator.

In a previous work [12], we investigated a wide region of the forcing-damping parameter space for this model, in which we found periodic, quasiperiodic, and chaotic behavior. Moreover, for weak dissipation we have observed a predominance of multistable behavior, displaying the coexistence of periodic and chaotic attractors, with a highly convoluted basin of attraction structure. From the point of view of operational safety, a suspension bridge must withstand a quite large variety of environmental wind conditions without too large maximum deflections of its roadbed. Hence, it is of paramount importance to know the set of initial conditions (in the phase space comprising the deformation of the roadbed and its time derivative) which leads to a midpoint beam deflection below a given threshold. This is known as a *safe basin*, its complement being the corresponding *exit basin*, or the set of initial conditions which ultimately lead to collapse [13].

If the safe basin has a smooth boundary, it suffices—for safety purposes—for an initial condition to be not closer than a numerical factor times the uncertainty to which these variables are measured. This numerical factor can be determined by empirical methods but should be of the order of unity. However, if the safe basin has a fractal boundary, besides exhibiting final-state sensitivity, it accesses extended regions of the phase space and thus possibly leading to a substantial shrinking in the size of the safe basin.

In this work, we consider the safe basin for the suspension bridge model of Refs. [2] and [11], and analyze the effect of the forcing amplitude and oscillation damping on the shape and size of the safe basin. In particular, we investigate the strong erosion of the safe basin due to the appearance of incursive fingers which rapidly decrease its relative area, rendering the operation of the bridge highly unsafe from this point of view, even if there is a positive measure set of safe initial conditions. The formation of these fingers is due to the accumulation of bands belonging to the safe basin, when its boundary intersects an invariant manifold of a saddle periodic orbit undergoing a homoclinic bifurcation.

The rest of this paper is organized as follows: in Section 2, we outline the dynamical model of the lowest transversal mode of a suspension bridge. Section 3 focuses on some aspects of its dynamical behavior, including the safe and exit basins, whereas Section 4 discusses the erosion of the safe basin and its mechanism. Section 5 contains our conclusions.

## 2. Suspension bridge model

A suspension bridge has a roadbed (elastic beam) sustained by a large number of hangers, which are steel cables attached to a main suspended cable. The roadbed is hinged in both ends to anchorage blocks, and the main cable is supported by high towers (Fig. 1). In this paper we neglect the deflections of the main cable, and consider the oscillations of the roadbed with a restoring force provided by the hangers. Let $x$ and $z$ be coordinates describing the vibrating roadbed along its length and width, respectively, whereas $u$ is the beam deflection along the transversal direction $y$, assuming a downward deflection as positive. Since we will consider only the transversal vibrations of the roadbed, we ignore any functional dependence of the deflections on $z$, so $u = u(x, t)$.

The hangers are supposed to be one-sided springs: they do not withstand compression efforts, but they oppose a linear restoring force when stretched, provided the deformations are small enough to be treated in the elastic regime,

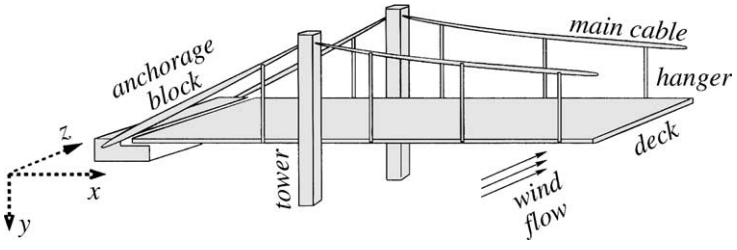


Fig. 1. Schematic figure of a suspension bridge.

without exceeding the rupture limit. Within these limits, the restoring force can be expressed as $-k'u^+$, where $k'$ is the spring constant and $u^+ = \max\{u, 0\}$. This leads to a piecewise linear and asymmetric stiffness: for downward deflections we take into account the combined response of the beam and stretched hangers, whereas, for upward deflections, only the beam elasticity is considered [2,11]. Moreover, we add a term $W(x)$ representing the proper weight of the beam and its loading.

The beam transversal vibrations are described by [11]

$$M\frac{\partial^2 u}{\partial t^2} + EI\frac{\partial^4 u}{\partial x^4} + \delta'\frac{\partial u}{\partial t} = -k'u^+ + W(x) + F(x,t), \tag{1}$$

where $M$ is the beam mass per unit length, $E$ is the Young modulus of the beam, and $I$ the moment of inertia of its transversal section. The dissipative effect is modelled by a viscous damping term $\delta' u_t$. The external force $F(x,t)$ represents the periodic driving effect of a Von Karman vortex street from wind impinging the bridge from the $z$-direction, and with a well-defined period $T = 2\pi/\omega'$:

$$F(x,t) = F_0(x)\sin(\omega' t). \tag{2}$$

The following boundary conditions are imposed

$$u(0,t) = u(L,t) = \left.\frac{\partial^2 u}{\partial x^2}\right|_{(0,t)} = \left.\frac{\partial^2 u}{\partial x^2}\right|_{(L,t)} = 0, \tag{3}$$

where $L$ is the length of the roadbed.

Because of the reasons explained in Section 1, we shall analyze only the lowest transversal harmonic of the bridge vibration

$$u(x,t) = y(t)\sin\left(\frac{\pi x}{L}\right), \tag{4}$$

where $y(t) = u(L/2,t)$ indicates the maximum deflection of the bridge roadbed, measured at its midpoint. Accordingly, we make a similar separation of variables for the other functions

$$W(x) = W'\sin\left(\frac{\pi x}{L}\right), \quad F_0(x) = B'\sin\left(\frac{\pi x}{L}\right). \tag{5}$$

Since the preloading $W$ is usually taken to be a constant value, the decomposition for $W(x)$, Eq. (5), should be intended as the lowest order term in the harmonic expansion of a constant function, which amounts to an error less than 10% [2].

Substituting these expressions into Eq. (1), the time evolution of the roadbed midpoint deflection turns out to be governed by an ordinary differential equation

$$M\frac{\mathrm{d}^2 y}{\mathrm{d}t^2} + \delta'\frac{\mathrm{d}y}{\mathrm{d}t} + EI\left(\frac{\pi}{L}\right)^4 y + k'y^+ = W' + B'\sin(\omega' t). \tag{6}$$

which, after defining the following non-dimensional spatial and temporal variables

$$\hat{x} = \frac{\pi x}{L}, \quad \hat{t} = \left(\frac{\pi}{L}\right)^2\sqrt{\frac{EI}{M}}t, \tag{7}$$

as well as the normalized parameters

$$\delta = \left(\frac{L}{\pi}\right)^2\frac{\delta'}{2\sqrt{EIM}}, \quad k = \left(\frac{L}{\pi}\right)^4\frac{k'}{EI}, \tag{8}$$

$$\omega = \left(\frac{L}{\pi}\right)^2\omega'\sqrt{\frac{M}{EI}}, \quad B = \left(\frac{L}{\pi}\right)^4\frac{B'}{EI}, \quad W = \left(\frac{L}{\pi}\right)^4\frac{W'}{EI}, \tag{9}$$

is rewritten as

$$y'' + 2\delta y' + my = W + B\sin(\omega t), \tag{10}$$

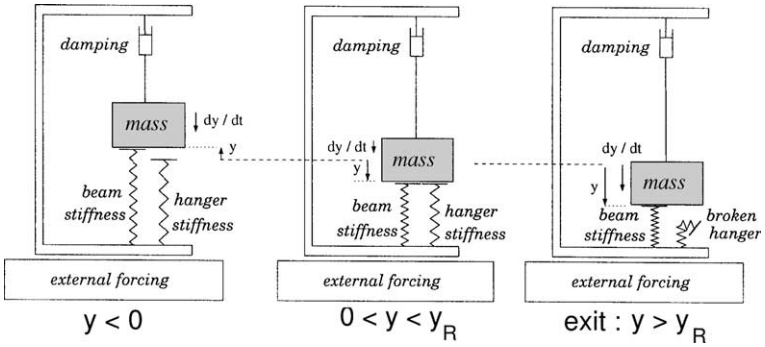


Fig. 2. One-dimensional oscillator with two springs, one of them with a clearance, equivalent to the suspension bridge transversal vibrations: (a) upward deflections, for which only the beam stiffness is acting, (b) downward deflections, for which both the beam and hanger stiffnesses occur and (c) rupture. The string in the upper part of the figure plays no role in the elastic response of the oscillator.

where the primes denote derivatives with respect to the scaled time, the hats on the variables being removed for ease of notation, and

$$m = \begin{cases} 1 & \text{if } y < 0, \\ (k+1) & \text{if } y > 0, \end{cases} \tag{11}$$

represents the piecewise-linear stiffness.

Fig. 2 shows a simple mechanical analogue of Eq. (10), as a externally driven and damped spring-mass one-dimensional system. The combined stiffness of the beam and hangers, provided the rupture limit is not achieved, acts only for positive deflections. This makes the system akin to oscillators with clearances, or discontinuities [5–10].

## 3. Safe and exit basins

We assume that the beam (and consequently the bridge) collapses if its midpoint deflection $y(t)$ exceeds some specified value $y_R$, the rupture deflection, which is related to the maximum allowed stress on the roadbed. In such a case, a crude model for the behavior when $y > y_R$ assumes that the restoring force provided by the hangers would disappear, so that the beam has only its proper weight (a non-smooth potential with discontinuous force, see Fig. 3(a)). However, it is too strong to assume that the restoring force could immediately vanish after $y = y_R$, since this force is continuously distributed along the beam, and after the roadbed collapses the hangers would (ideally) disrupt according to their distances to the midpoint.

A more realistic, but still a phenomenological model, would be represented by an exponential decrease of the effective force on the roadbed for $y > y_R$ (a smooth potential with a piecewise-smooth continuous effective force):

$$F_{\text{eff}}(y) = W - (k+1)y_R \exp[-\beta(y - y_R),] \quad (y > y_R), \tag{12}$$

where we have adopted $\beta = 10$ for a faster convergence (see Fig. 3(b)).

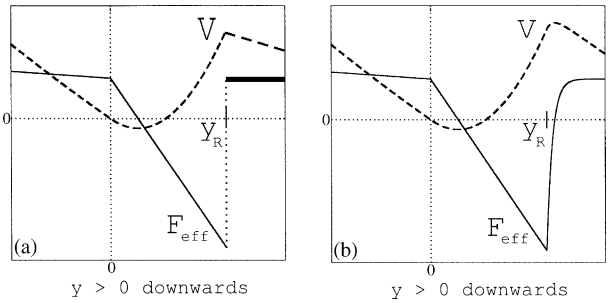


Fig. 3. Restoring force (full line) and the corresponding effective potential (dashed line) as a function of the vertical bridge deflection $y$: (a) simple rupture and (b) exponentially decreasing rupture.

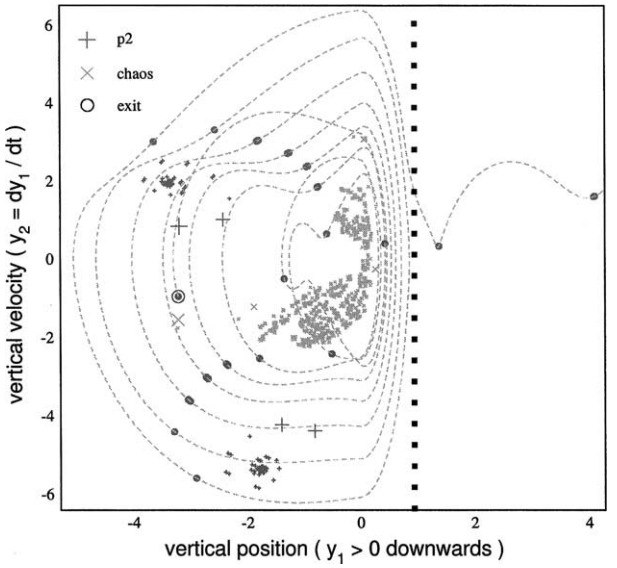


Fig. 4. Phase portrait (vertical deflection versus vertical velocity) for the suspension bridge model (10), with $W = 1$, $k = 50$, $\omega = 4.0$, $B = 3.0$, $\delta = 0.05$ and $y_R = 0.775$. Three initial conditions are used, leading to a period-2 attractor (time-$T$ map points are marked "+"), a chaotic attractor (points marked "x"), and an escaping trajectory (points are marked "o"). The corresponding continuous-time trajectories are represented by dashed lines. The filled squares represent the critical line for collapse.

The non-smoothness of the vector field (10) leads to a complex dynamics for the bridge oscillations, in the sense that one expects the coexistence of various attractors, both periodic and chaotic, with an involved basin structure [12], not necessarily but very often of a fractal nature. The introduction of a rupture prescription like Eq. (12) introduces a novel feature which enhances the complexity of the system, for the bridge collapse can be considered as a kind of "attracting behavior". This does not correspond necessarily to a new attractor, since in principle any attractor would lead to collapse, if $y > y_R$.

The rupture condition, in the phase space $y \times \dot{y}$, is represented by a straight line $y = y_R$, such that an initial condition will ultimately lead to collapse if the trajectory starting from it crosses the critical line in some point. If the basin of any attractor intersects this line, it is probable that some initial condition, which would otherwise asymptote to the attractor, will eventually escape for $y > y_R$. This can occur both for basins of either periodic or chaotic attractors. Fig. 4 shows such a situation, in which there is coexistence of a period-2 attractor (stable focus) and a chaotic attractor in the phase space (vertical bridge deflection versus time-rate of deflection). In this figure, it is also shown a trajectory, starting from an initial condition lying in the basin of the period-2 attractor, which escapes after reaching $y > y_R$. The points shown in Fig. 4 result from a stroboscopic (time-$T$) map from the continuous time flow [2]. Chaos is characterized through the formation of a topological horseshoe for the invariant attracting set [5]. Fig. 5 shows segments of the stable and unstable manifolds emanating from a saddle fixed point embedded in the chaotic attractor of Fig. 4. The formation of a topological horseshoe is inferred from the existence of homoclinic intersections of these manifolds in phase space.

What ultimately determines whether or not an initial condition leads to a collapse is not to what basin of attraction it belongs, but rather whether or not the corresponding transient behavior leads to $y \geqslant y_R$. This essential difference leads to the concept of a *safe basin*, which is the set of initial conditions that do not lead to collapse, i.e., the corresponding transient trajectories have $y(t) < y_R$ for all times. Its complement in the phase plane is the corresponding *exit basin*. This definition is operational in the sense that it provides the algorithm for its obtention. Let us consider a bounded region of the phase plane and cover it with a fine grid of points, and use each point as an initial condition for evolving the flow (10) for a large time $t_{max}$. If, for $0 < t < t_{max}$ no orbit point has $y(t) \geqslant y_R$, then very probably this initial condition is safe and it is painted gray; otherwise we stop integrating just after the condition $y > y_R$ is fulfilled by the trajectory, and we mark the initial condition as a dark pixel. The gray and dark regions are numerical approximations to the safe and exit basins, respectively.

[2] We have numerically solved (10) by using a 12th order Adams method (from the LSODA package [14]).

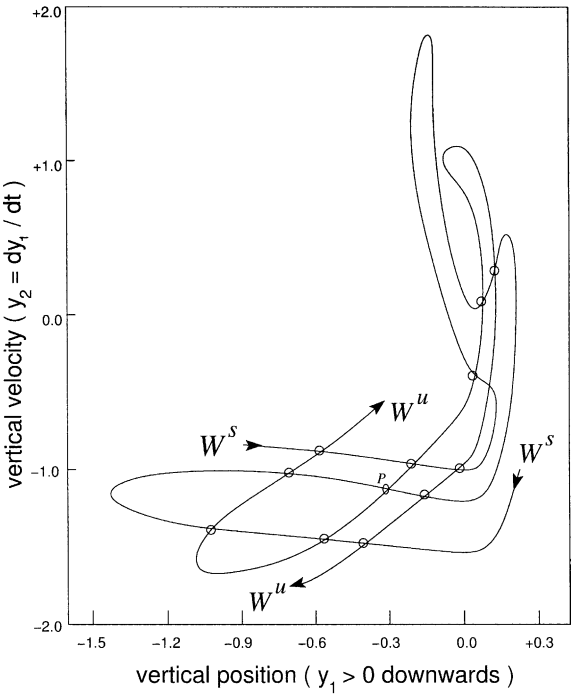


Fig. 5. Stable and unstable manifolds emanating from a fixed point embedded in the chaotic attractor shown in Fig. 4. The existence of homoclinic intersections signals the formation of a topological horseshoe in the phase plane.

Fig. 6 shows a sequence of such plots for a fixed value of the damping coefficient $\delta$ and nine values of the forcing amplitude $B$. The relative area of the safe basin in the region under consideration, denote here as $f$, is approximated by the ratio between the number of gray pixels and the total number of pixels covering the phase-space region selected out for analysis. This region is supposed to cover all safe initial conditions. We observed that the area $f$ decreases, from about 32% to virtually zero as the wind forcing increases. This is consistent with the increase of the oscillation amplitudes as the forcing builds up, what turns a collapse more frequently observed for "typical" initial conditions.

## 4. Erosion of the safe basin

The decrease of the relative safe basin area with the forcing amplitude is often called basin erosion, and can be illustrated in Fig. 7(a). For forcing amplitudes less than a critical value (about 2.5 for the parameters used in Fig. 7(a)) there is no erosion at all, and this is followed by a decrease which can be reasonably fitted as a power law $f(B) = C_1 B^{-\gamma_1}$,where $C_1 = 2.9$ and $\gamma_1 = 2.3$. This scaling persists up to another critical amplitude, followed by an abrupt fall and vanishing of the safe area. This non-trivial behavior can be partially understood by considering the corresponding bifurcation diagram for the vertical position versus the forcing amplitude (Fig. 7(b)).

There is a period-1 stable orbit of the stroboscopic map, for small forcing amplitudes, corresponding to a primary non-linear resonance between the natural and forcing frequencies. As the driving amplitude increases to $B \approx 1.8$ this orbit undergoes a subharmonic period-doubling cascade to chaos, with accumulation at $B \approx 2.7$. The chaotic attractor disappears at $B \approx 3.8$ due to a crisis, i.e., it collides with an unstable periodic orbit. For a small window between $B = 2.0$ and 2.5 there is another period-3 coexisting attractor, born through a saddle-node bifurcation, and which also undergoes a similar period-doubling cascade, disappearing beyond another crisis. The decrease of the safe area occurs continuously and it increases roughly in the parameter region where a chaotic attractor exists, and the sudden vanishing of the safe area coincides with the crisis which destroys the chaotic attractor. For $B > 2.7$ one sees an apparently fractal boundary separating the safe and exit basins. This structure leads to a sensitivity to the final state, meaning that an increase in the accuracy of the initial condition leads to only a modest increase in our ability to predict in which basin the initial condition is [19].

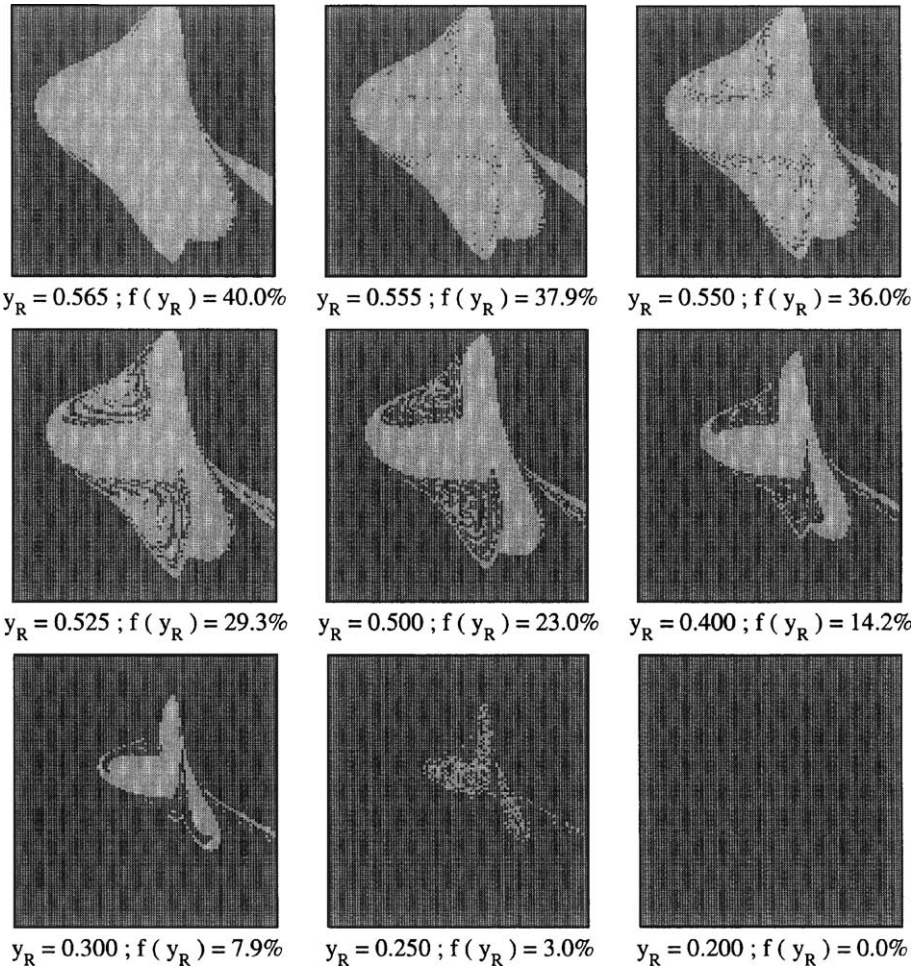


Fig. 6. Phase portraits showing the safe (gray) and exit (dark) basins, for $W = 1$, $k = 50$, $\omega = 4.0$, $\delta = 0.10$, $y_R = 0.5$, and nine values of the forcing amplitude $B$. The normalized safe area is also indicated in the panels.

It should be emphasized that the basin erosion process we are dealing with in this paper is somewhat different from the extensively studied problem of safe basins of a driven oscillator under the potential

$$V(x) = \frac{1}{2}x^2 - \frac{1}{3}x^3, \tag{13}$$

which models, for example, the rolling motion of a ship under ocean waves [13,15–18]. The safe basin there is the set of initial conditions which do not lead to the capsizing of the ship ($x \to -\infty$). However, in this case, the safe basin actually corresponds either to a basin of some bounded attractor or to the union of the basin of bounded attractors (the escape could be viewed as an attractor at infinity). The observed fast erosion of the safe basin can be interpreted as a result of a homoclinic tangency of the stable and unstable manifolds of the hilltop unstable saddle orbit. The erosion is continuous but there are discontinuous changes whose rate is determined by the manifold intersections following a homoclinic tangency [15].

On the other hand, in the problem of the bridge collapse we have chosen the rupture deformation in a rather arbitrary way, such that the critical line in the phase space, given by $y = y_R$ intercepts one or more basins of attraction. Hence, we should not expect, in general, that the safe basin coincides with some basin of attraction. The interpretation of this result should be looked for in the properties of the transient behavior of trajectories in phase space. As far as the critical line intercepts some basin, it may well happen that an initial condition, even far from this line, can generate a transient trajectory which hits the critical line and exits, thus leading to collapse.

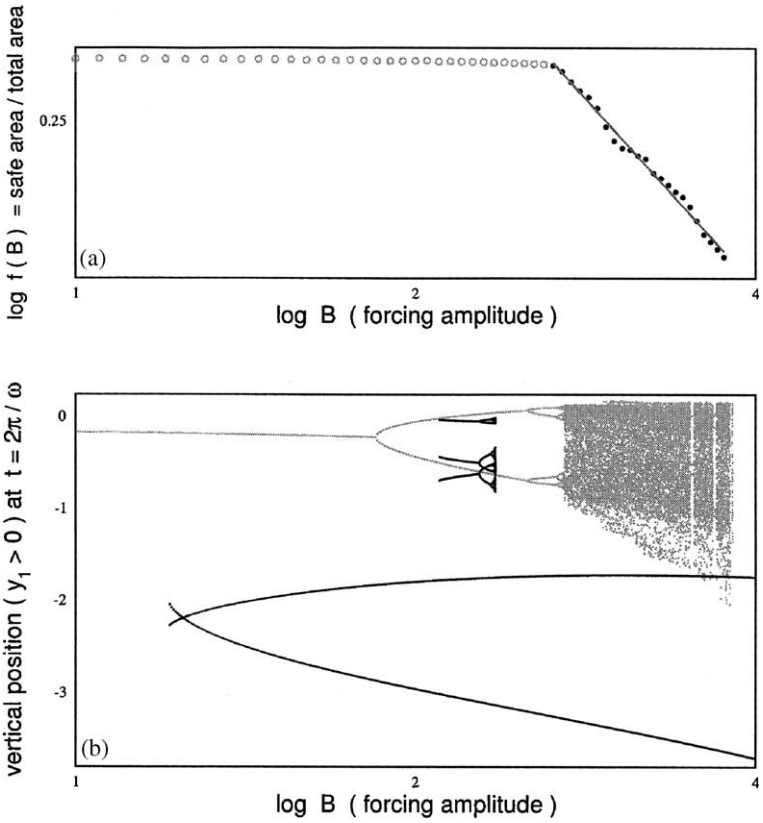


Fig. 7. (a) Relative safe area as a function of the forcing amplitude, for the same parameters as the previous figure. The straight line shown for $2.65 < B < 3.75$ is a least-squares fit for the points marked as full circles. (b) Bifurcation diagram for the vertical position (of the time-$T$ map) versus the forcing amplitude, showing coexistence of periodic and chaotic attractors.

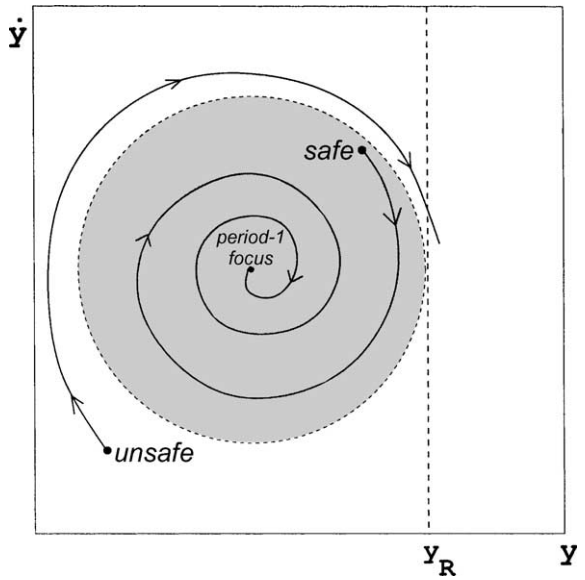


Fig. 8. Schematic figure of a phase portrait containing only one period-1 attractor and two initial conditions, one belonging to the safe basin and other leading to rupture. The safe basin is depicted as a gray circle touching the critical line for rupture $y = y_R$.

Although no complete theory exists for transient behavior, some facts can help us to grasp a picture of the process leading to basin erosion. Let us first imagine a simple situation: a unique basin of a period-1 stable focus at $(y^*, \dot{y}^* = 0)$, intercepting the critical line (see Fig. 8). A typical initial condition in this basin will spiral towards the focus with a time rate given by the eigenvalues of the linearized map, evaluated at the equilibrium point. Let us suppose for simplicity that the eigenvalues are equal so that the projection of the transient orbit is an equilateral spiral converging to $(y^*, 0)$. A transient trajectory would hit the critical line only if the initial condition is placed at a distance greater than $|y_R - y^*|$.The safe basin would be a circle centred at $(y^*, 0)$ (or a part of it) touching the critical line.

In fact, in the first panel of Fig. 6, corresponding to a value of $B$ for which there is a single period-1 focus near the origin, the safe basin is a closed and apparently smooth curve touching the critical line (the rightmost margin). The fast decrease of the safe area, beginning at $B \approx 2.70$, is followed by the formation of incursive fingers (seen from the fourth panel of Fig. 6) in a similar way to those observed in the problem of capsizing ship [13].

Fractal basin boundaries of attractors are naturally incursive, in the sense that they are related to homo and heteroclinic intersections of stable and unstable manifolds of saddle periodic orbits of the system. Since those intersections map one to another ad infinitum, the manifolds present a convoluted structure that extends through a wide portion of the phase space. The transient orbits near such a fractal basin boundary would be as convoluted as the boundary itself, so they are expected to cross the critical line very often, increasing dramatically the number of unsafe initial conditions. In this case the erosion of the safe basin is also related, but in a less obvious way, to fractal basin boundaries of attractors.

The presence of a homoclinic tangency signals the transformation of a basin boundary of a *non-chaotic* attractor, from smooth to fractal, as it has been shown for the forced Duffing equation [20]. When the forcing amplitude is further increased, chaotic motion sets in, corresponding to the evolution of the homoclinic tangencies, with a persistence of the fractal basin boundaries. This fact may suggest why the safe basin erosion occurs slightly before the chaotic attractor sets in (see Fig. 7(b)). The sudden disappearance of the chaotic attractor for $B \approx 3.8$, following a crisis, leads to the vanishing of the safe area, since the attractor no longer exists and is replaced by a long chaotic transient which visits for some time the remnant of the chaotic attractor and goes far away from it, eventually crossing the critical line.

A qualitatively similar picture emerges when the variable parameter is the damping instead of the forcing amplitude. Fig. 9 shows a sequence of safe basins for decreasing damping coefficients, also showing basin erosion due to the presence of incursive fractal fingers. The normalized safe basin area is plotted in Fig. 10 as a function of increasing damping, which exhibits a power-law fit for small damping: $f(\delta) = C_2\delta^{-\gamma_2}$, where $C_2 = 3.8$ and $\gamma_2 = 1.22$. In the ship capsizing problem, the appearance of incursive fingers, as the damping coefficient is varied, is also related to homoclinic intersections, and can even be predicted on the basis of the Melnikov criterion [13]. For the suspension bridge model the transient trajectories can be very long for small damping, and thus it becomes more probable (when the boundaries are fractal) that they cross the critical line and escape.

We can understand the formation of these incursive fingers by considering the effects of the dynamics on some partition line $\Gamma$ separating two regions in phase space, when this partition line intersects some invariant manifold of an unstable fixed point in phase space (for the stroboscopic map). This partition line does not need necessarily to be a basin boundary segment, and actually it is not, since, as we have seen, the safe basin in general does not coincide with the basin of some attractor in the bridge problem. In this case, a partition line is the boundary of a safe basin. The conditions under which there are incursive fingers are: (i) there is a homoclinic bifurcation in the bridge dynamics; (ii) the safe basin boundary intercepts an invariant manifold of the periodic orbit $P$ that underwent this homoclinic bifurcation.

Since the stroboscopic (time-$T$) map $\mathscr{F}$ is invertible, we can compute both the forward and backward images of points and sets in the phase plane. Under the backward images of the map, the iterations of the partition line $\Gamma$ intersecting the unstable manifold of $P$, i.e.,. $\mathscr{F}^{-n}(\Gamma)$, approaches $P$ as time goes to infinity, in such a way that (see Fig. 11): (i) the intersection points between the unstable manifold and the boundary of the set $\Gamma$ converge exponentially fast, according to the corresponding unstable eigenvalue of the linearized map at $P$; (ii) the lengths of the lobes, or incursive fingers, increase exponentially to compensate for the decreasing of their widths, and the fingers themselves tend to follow the stable manifold of $P$. The union of all images of $\Gamma$ is a curve which oscillates as it approaches the unstable fixed point, such that the segments of the safe basin boundary will become extremely thin filaments accumulating on the stable manifold of $P$ [21].

Finally, Fig. 12 presents a sequence of safe basins when the rupture deformation, $y_R$, is varied. The presence of incursive fractal fingers is also observed, and causes safe basin erosion as the critical line approaches the origin, what is already expected since a nearby critical line would intercept many more trajectories than a farther line would. The corresponding reduction of the safe area also obeys a power-law behavior in a certain range of the rupture deformation (see Fig. 13): $f(y_R) = C_3 y_R^{-\gamma_3}$, with $C_3 = 1$, and $\gamma_3 = 1.97$.

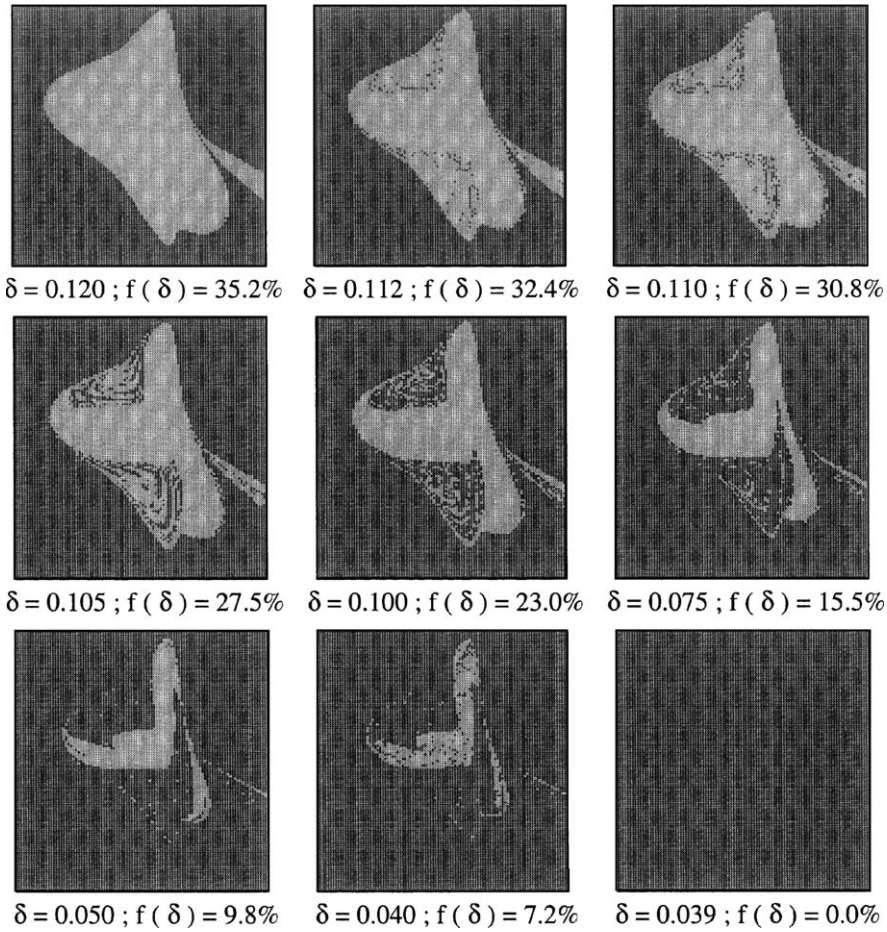


Fig. 9. Phase portraits showing the safe (gray) and exit (dark) basins, for $W = 1$, $k = 50$, $\omega = 4.0$, $B = 3.0$, $y_R = 0.5$, and nine values of the damping coefficient $\delta$. The relative safe area is also indicated in the panels.

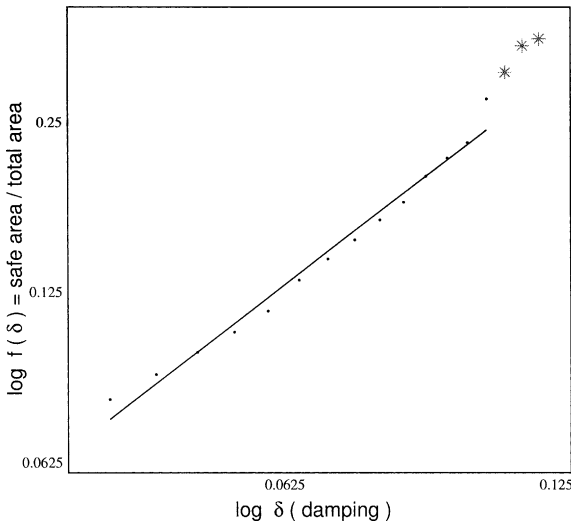


Fig. 10. Safe area as a function of the damping coefficient, for the same parameters as the previous figure. The straight line for $0.04 < \delta < 1.05$ is a least-squares fit for the points marked as full circles.

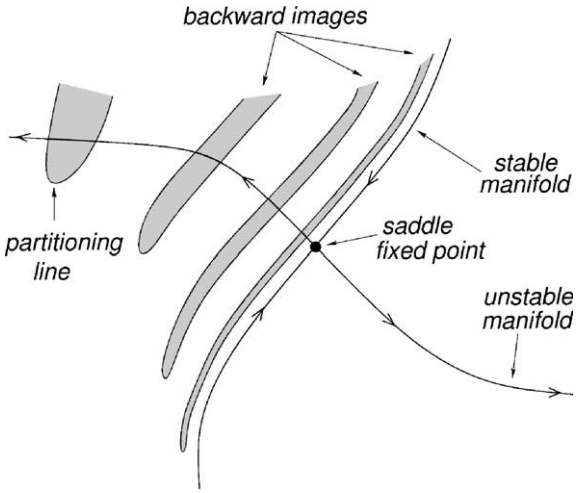


Fig. 11. Schematic figure showing the formation of incursive fingers of the safe basin, resulting from the backward images of a partitioning line which intercepts the unstable manifold of a fixed point of the time-$T$ map.

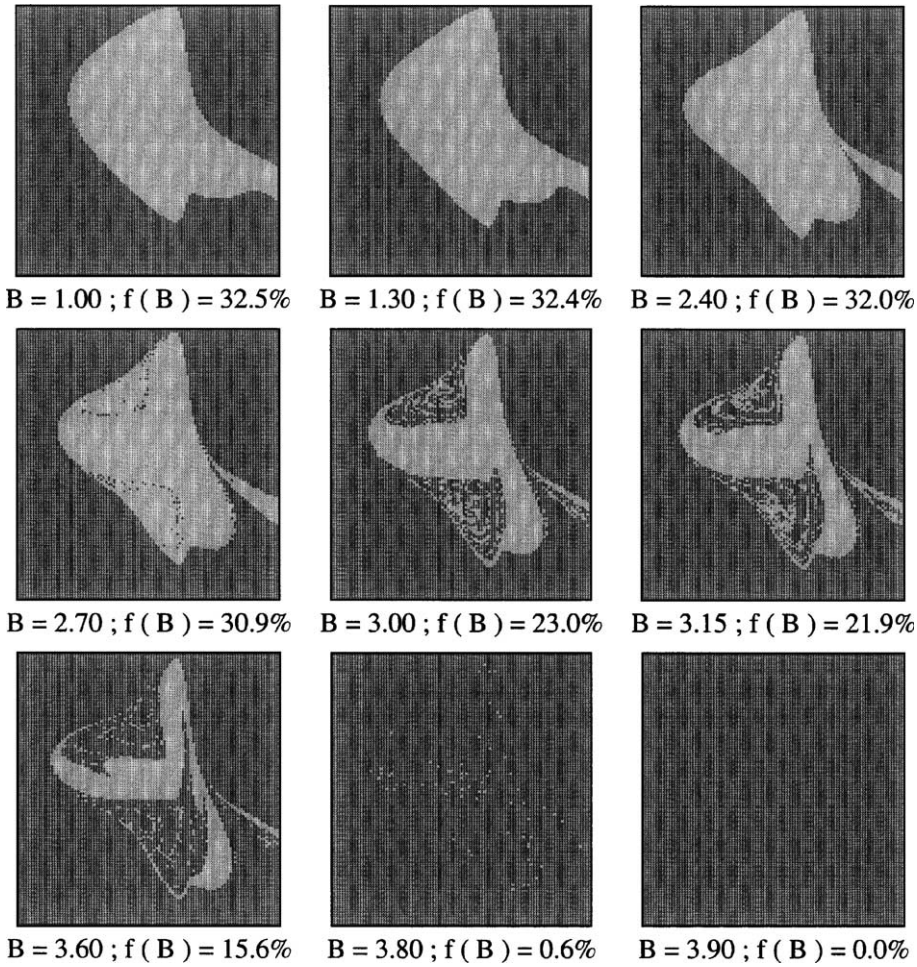


Fig. 12. Phase portraits showing the safe (gray) and exit (dark) basins, for $W = 1$, $k = 50$, $\omega = 4.0$, $B = 3.0$, $\delta = 0.100$, and nine values of the rupture deformation $y_R$. The relative safe area is also indicated in the panels.

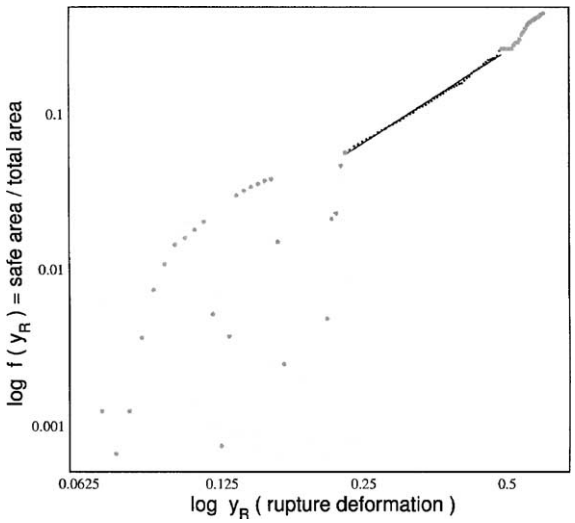


Fig. 13. Safe area as a function of the rupture deformation, for the same parameters as in the previous figure. The straight line for $0.23 < y_R < 0.49$ is a least-squares fit for the points marked as full circles.

## 5. Conclusions

The renewal of interest in the Tacoma Narrows bridge failure problem is due to the general awareness of the key role played by non-linearity in its dynamical behavior. Striking non-linear features already appear when we consider the dynamics of a single, lowest-order transversal vibration mode. Other modes, as torsional ones, have been shown to present a similarly rich behavior [22]. The weakly damped and forced dynamical system presents multistable behavior with many coexistent attractors, both periodic and chaotic, with a complicated basin structure. Hence, we can call the suspension bridge a complex system in the sense that: (i) it is composed of many parts that are interrelated in a non-trivial manner; (ii) it has both ordered and random behaviors; and (iii) it exhibits a hierarchy of structures over a wide range of lengths [23]. External noise is able to drive the system off a given basin and make it jump to another one, what can cause structural damage due to the resulting amplitude jumps.

We have assumed that, if the bridge maximum deformation exceeds some threshold it collapses. In view of that, the collapse depends not so much on the character of the coexistent attractors but instead on the transient behavior. We have studied in this paper the sets of initial conditions which do not lead to collapse, or safe basins, and got numerical evidence that there is a sharp reduction of the area of this safe basin as a system parameter is varied. We have considered the forcing amplitude, the damping coefficient and the rupture deformation as the variable parameters. The safe basin is determined basically by the transient behavior of orbits belonging to one or more coexisting basins of attraction. Fractal basin boundaries lead to transient orbits crossing more frequently the critical line of rupture in the phase space and, as a consequence, there is a substantial erosion of the safe basin, with a typical presence of incursive fingers. These fingers, on the other hand, result from successive intersections of the safe basin boundary with an invariant manifold of a saddle periodic orbit in phase space.

## Acknowledgements

This work was made possible by partial financial support from the following Brazilian government agencies: CNPq, CAPES, Fundação Araucária, and FAPESP.

## References

[1] Billah KY, Scanlan RH. Resonance, Tacoma Narrows bridge failure and undergraduate Physics textbooks. Am J Phys 1991;59:118–24.

[2] Lazer AC, McKenna PJ. Large amplitude periodic oscillations in suspension bridges: some new connections with nonlinear analysis. SIAM Rev 1990;58:537–78.

[3] Images of the disaster are available in the website http://cee.carleton.ca/Exhibits/TacomaNarrows/, taken from the 20-minute silent movie.
[4] Nayfeh AH, Mook DT. Nonlinear oscillations. New York: Wiley-Interscience; 1979.
[5] Shaw SW, Holmes PJ. A periodically forced piecewise linear oscillator. J Sound Vibrat 1983;90:29–155.
[6] Kim YB, Noah ST. Stability and bifurcation analysis of oscillators with piecewise-linear characteristics: a general approach. J Appl Mech 1991;58:545–53.
[7] Blazejczyk-Okulewska B, Czolczynski K, Kapitaniak T, Wojewoda J. Chaotic mechanics in systems with friction and impacts. Singapore: World Scientific; 1999.
[8] Blazejczyk-Okulewska B. Study of the impact oscillator with elastic coupling of masses. Chaos, Solitons & Fractals 2000;11:2487–92.
[9] Wiercigroch M, DeKraker B. Applied nonlinear dynamics and chaos of mechanical systems with discontinuities. Singapore: World Scientific; 2000.
[10] Wiercigroch M. Modelling of dynamical systems with motion dependent discontinuities. Chaos, Solitons & Fractals 2000;11:2429–42.
[11] Doole SH, Hogan SJ. A piecewise linear suspension bridge model: nonlinear dynamics and orbit continuation. Dynam Stab Syst 1996;11:19–47.
[12] Freitas MST, Viana RL, Grebogi C. Multistability, basin boundary structure, and chaotic behavior in a suspension bridge model. Int J Bif Chaos, in press.
[13] Thompson JMT, Rainey RCT, Soliman MS. Ship stability criteria based on chaotic transients from incursive fractals. Phil Trans R Soc Lond A 1990;332:149–67.
[14] Hindmarch AC. ODEPACK: a systematized collection of ODE solvers. In: Stepleman RS et al., editors. Scientific computing. Amsterdam: North-Holland; 1983.
[15] Soliman MS, Thompson JMT. Global dynamics underlying sharp basin erosion in nonlinear driven oscillators. Phys Rev A 1992; 45:3425–31.
[16] Soliman MS. Fractal erosion of basins of attraction in coupled nonlinear systems. J Sound Vib 1995;182:727–40.
[17] Kükner A. A view on capsizing under direct and parametric wave excitation. Ocean Engng 1998;25:677–85.
[18] Senjanovic I, Parunov J, Cipric G. Safety analysis of ship rolling in rough sea. Chaos, Solitons & Fractals 1997;4:659–80.
[19] McDonald SW, Grebogi C, Ott E, Yorke JA. Fractal basin boundaries. Physica D 1985;17:125–53.
[20] Moon FC, Li G-X. Fractal basin boundaries and homoclinic orbits for periodic motion in a two-well potential. Phys Rev Lett 1985;55:1439–42.
[21] Pentek A, Toroczkai Z, Tel T, Grebogi C, Yorke JA. Fractal boundaries in open hydrodynamical flows: signatures of chaotic saddles. Phys Rev E 1995;51:4076–88.
[22] Doole SH, Hogan SJ. Nonlinear dynamics of the extended Lazer–McKenna bridge oscillation model. Dynam Stab Syst 2000; 15:43–58.
[23] Feudel U, Grebogi C. Multistability and the control of complexity. Chaos, Solitons & Fractals 1997;7:597–604.